Application of the penetration theory for gas - Liquid mass transfer without liquid bulk

van Elk, E. P.; Knaap, M. C.; Versteeg, G. F.

Published in:
Chemical Engineering Research and Design

DOI:
10.1205/cherd06066

Publication date:
2007

APPLICATION OF THE PENETRATION THEORY FOR GAS–LIQUID MASS TRANSFER WITHOUT LIQUID BULK

Differences with Systems with a Bulk

E. P. van Elk[1,*], M. C. Knaap[2] and G. F. Versteeg[1]

[1]Procede Twente BV, Enschede, The Netherlands.
[2]Shell Research and Technology Centre Amsterdam, Amsterdam, The Netherlands.

Abstract: Frequently applied micro models for gas–liquid mass transfer all assume the presence of a liquid bulk. However, some systems are characterized by the absence of a liquid bulk, a very thin layer of liquid flows over a solid surface. An example of such a process is absorption in a column equipped with structured packing elements. The penetration model was slightly modified, so that it can describe systems without liquid bulk. A comparison is made between the results obtained with the modified model and the results that would be obtained when applying the original penetration theory for systems with liquid bulk. Both physical absorption and absorption accompanied by first and second order chemical reaction have been investigated. It is concluded that the original penetration theory can be applied for systems without liquid bulk, provided that the liquid layer has sufficient thickness ($\delta > d^*_{pen}$). For packed columns this means, in terms of Sherwood number, $Sh \geq 4$. In case of a 1,1-reaction with $Ha > 0.2$ an additional second criterion is $Sh \geq 4\sqrt{D_b/D_a}$ For very thin liquid layers ($Sh < 4$ or $Sh < 4\sqrt{D_b/D_a}$), the original penetration model may give erroneous results, depending on the exact physical and chemical parameters, and the modified model is required.

Keywords: penetration theory; mass transfer; film; liquid layer; packed columns; structured packing.

*Correspondence to:
Dr E.P. van Elk, Procede Twente BV, P.O.BOX 328 7500, AH Enschede, The Netherlands,
E-mail: edwin.vanelk@procede.nl

DOI: 10.1205/cherd06066

0263–8762/07/$30.00 + 0.00

Chemical Engineering Research and Design

Trans IChemE, Part A, April 2007

INTRODUCTION

Mass transfer from a gas phase to a liquid phase proceeds via the interfacial area. Micro models are required to model this interphase transport of mass that often takes place in combination with a chemical reaction.

Frequently applied micro models are the stagnant film model in which mass transfer is postulated to proceed via stationary molecular diffusion in a stagnant film of thickness δ (Whitman, 1923), the penetration model in which the residence time θ of a fluid element at the interface is the characteristic parameter (Higbie, 1935), the surface renewal model in which a probability of replacement is introduced (Danckwerts, 1951) and the film-penetration model which is a two-parameter model combining the stagnant film model and the penetration model (Dobbins, 1956; Toor and Marchello, 1958).

All micro models mentioned above assume the presence of a well mixed liquid bulk. This may limit the application of these models to systems where a liquid bulk is present, for example absorption in a tray column or mass transfer in a stirred tank reactor. The question arises whether it is also possible to apply the micro models for systems where no liquid bulk is present, for example absorption in a column with structured or random packing elements, where thin liquid layers flow over the packing.

In this paper, the penetration model approach is adapted, so that it can describe systems without a liquid bulk. Next, a comparison is made between the results obtained with the modified model and the results that would be obtained when applying the original penetration theory for systems with a liquid bulk.

THEORY

Introduction

The problem considered is gas–liquid mass transfer followed by an irreversible first or second order reaction:

$$A(g) + \gamma_b B(l) \longrightarrow \gamma_c C(l) + \gamma_d D(l) \qquad (1)$$

with the following overall reaction rate equation:

$$R_a = k_R[A][B]^n \qquad (2)$$

where $\gamma_b = n = 0$ in case of a first order reaction and $\gamma_b = n = 1$ in case of a second order reaction.

The mathematical model used is based on the following assumptions:

(1) Mass transfer of component A takes place from the gas phase to a liquid layer that flows over a vertical contact surface (i.e., a packing or a reactor wall).
(2) The mass transfer in the gas phase is described with the stagnant film model. The conditions are chosen so that the gas phase mass transfer is no limiting factor.
(3) The mass transfer in the liquid phase is described according to the penetration model approach.
(4) The reaction takes place in the liquid phase only.
(5) The liquid phase components are non-volatile.
(6) Axial dispersion in the liquid layer can be neglected.
(7) The velocity profile in the liquid layer is either plug flow or a fully developed parabolic (laminar flow).
(8) Temperature effects on micro scale are neglected.

Higbie Penetration Model

First, the standard penetration model is discussed (Figure 1). The phenomenon of mass transfer accompanied by a chemical reaction is governed by the equations:

$$\frac{\partial[A]}{\partial t} = D_a \frac{\partial^2[A]}{\partial x^2} - R_a \tag{3}$$

$$\frac{\partial[B]}{\partial t} = D_b \frac{\partial^2[B]}{\partial x^2} - \gamma_b R_a \tag{4}$$

To permit a unique solution of the non-linear partial differential equations (3) and (4) one initial (5) and two boundary conditions (6) and (7) are required:

$$t = 0 \text{ and } x \geq 0: [A] = [A]_{l,bulk},\ [B] = [B]_{l,bulk} \tag{5}$$

$$t > 0 \text{ and } x = \infty: [A] = [A]_{l,bulk},\ [B] = [B]_{l,bulk} \tag{6}$$

$$J_a = -D_a \left(\frac{\partial[A]}{\partial x}\right)_{x=0} = k_g \left([A]_{g,bulk} - \frac{[A]_{x=0}}{m_a}\right)$$

$$\left(\frac{\partial[B]}{\partial x}\right)_{x=0} = 0 \tag{7}$$

Species C and D do not need to be considered because, due to the irreversibility of the reaction (1), they do not influence the mass transfer. Assuming that the mixture density is not affected, also the total flow of the is not affected.

Penetration Model for Systems Without Liquid Bulk

In this section it is assumed that mass transfer takes place from a continuous gas phase to a liquid layer that flows down over a vertical contact surface (Figure 2). The model can however be modified easily to apply for non-vertical surfaces or for systems without contact surface.

Mass transport in the x direction takes place by diffusion, as is the case with the penetration model. Mass transport in the vertical (y) direction takes place primarily due to the flow in the liquid layer over the contact surface. The contribution of diffusion or axial dispersion to the mass transport is neglected.

$$v_y \frac{\partial[A]}{\partial y} = D_a \frac{\partial^2[A]}{\partial x^2} - R_a \tag{8}$$

$$v_y \frac{\partial[B]}{\partial y} = D_b \frac{\partial^2[B]}{\partial x^2} - \gamma_b R_a \tag{9}$$

Please note that these equations are similar to the penetration model [equations (3) and (4)]. The vertical velocity v_y and the vertical position y have replaced the time t.

To permit a unique solution of the non-linear partial differential equations (8) and (9) one boundary condition (10) and two boundary conditions (11) and (12) are required:

$$y = 0 \text{ and } x \geq 0: [A] = [A]_{l,0}, [B] = [B]_{l,0} \tag{10}$$

$$y > 0 \text{ and } x = \delta: \frac{\partial[A]}{\partial x} = 0, \frac{\partial[B]}{\partial x} = 0 \tag{11}$$

$$J_a = -D_a \left(\frac{\partial[A]}{\partial x}\right)_{x=0} = k_g \left(\frac{[A]_{g,bulk} - [A]_{x=0}}{m_a}\right)$$

$$\left(\frac{\partial[B]}{\partial x}\right)_{x=0} = 0 \tag{12}$$

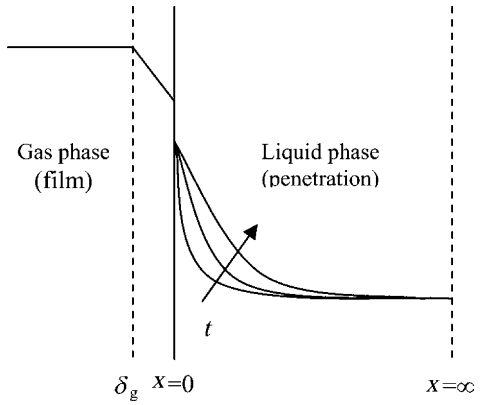

Figure 1. Penetration model for systems with liquid bulk.

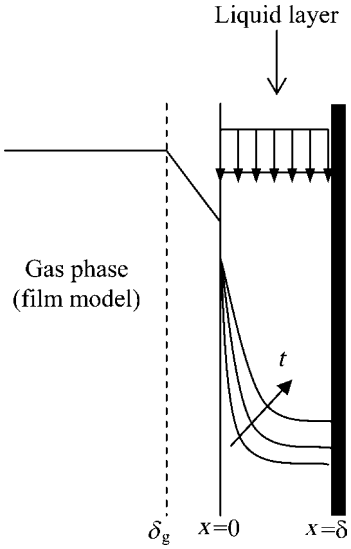

Figure 2. Penetration model for systems without liquid bulk.

Please note that the boundary condition for $x = \infty$ has been replaced by a boundary condition for $x = \delta$ (11). This boundary condition is a mathematical formulation for the fact that no species can diffuse through the solid surface.

Velocity Profile

The velocity profile, required to solve the model, is limited by two extremes:

(1) Plug flow, the velocity v_y is independent of position x.
(2) Laminar flow with no-slip boundary condition, the velocity v_y at the wall is zero. Assuming a parabolic velocity profile v_y can be calculated from

$$v_y = v_{max}\left(1 - \left(\frac{x}{\delta}\right)^2\right) \tag{13}$$

The maximum velocity v_{max} is found at the gas–liquid interface and can be calculated from

$$v_{max} = \frac{\rho g \delta^2}{2\mu} \tag{14}$$

The most likely situation is that at $t = 0$, the velocity profile is a plug flow profile. At $t > 0$ the velocity profile gradually changes from plug flow to parabolic. The actual (average) mass transfer flux between $t = 0$ and $t = \theta$ will be in between the mass transfer flux for plug flow and for parabolic velocity profile.

Mass Transfer Flux

The mass transfer flux is calculated as the average flux over the contact time θ (penetration model) or the contact length L (layer model):

$$J_{a,bulk} = \frac{1}{\theta}\int_0^\theta -D_a\left(\frac{\partial[A]}{\partial x}\right)_{x=0} dt \tag{15}$$

$$J_{a,\,layer} = \frac{1}{L}\int_0^L -D_a\left(\frac{\partial[A]}{\partial x}\right)_{x=0} dy \tag{16}$$

Numerical Treatment

The approach used to solve the model equations is based on the method presented by Versteeg *et al.* (1989). The special error-function transformation used by Versteeg *et al.* was not implemented, because this can only be applied on systems with a liquid bulk.

RESULTS

Introduction

The main objective of this paper is to investigate the differences between the results of the penetration model for systems with liquid bulk and the results of the modified model for systems where a thin liquid layer flows over a vertical contact surface.

Three different kinds of absorption have been investigated: physical absorption, absorption and irreversible 1,0 reaction and finally absorption and irreversible 1,1 reaction. Both plug flow and parabolic velocity profiles in the liquid layer were studied. All main parameters ([A], [B], D_a, D_b, k_R, δ, k_l, m_a, v_{max}) have been varied over a wide range.

It was found that most results could be summarised into only a few plots, using dimensionless numbers. The important dimensionless numbers used are

$$\eta = \frac{J_{a,layer}}{J_{a,bulk}} \tag{17}$$

$$X_i = \frac{\delta}{d_{peni}} = \frac{\delta}{\sqrt{4D_i\theta}} \tag{18}$$

$$Ha = \frac{\sqrt{k_R[B]^n D_a}}{k_l} \tag{19}$$

$$Sat = \frac{[A]_l^0}{m_a[A]_g} \tag{20}$$

Physical Absorption

First consider physical absorption ($k_R = 0$). The analytical solution of the absorption flux for the penetration model is given by

$$J_{a,bulk} = k_l(m_a[A]_g - [A]_l) \tag{21}$$

As a basecase, the following conditions were taken: $k_l = 5 \times 10^{-5}$ m s^{-1}, $m_a = 0.5$, $[A]_g = 100$ mol m^3, $D_a = 1 \times 10^{-9}$ m^2 s^{-1}, plug flow velocity in layer with $v_y = 0.1$ m s^{-1}. The corresponding penetration depth (d_{pen}) is 45 μm. The dimensionless mass transfer flux found with the modified model is given for layers of different thickness in Table 1.

The results presented in Table 1 are generalized by conversion in a dimensionless mass transfer efficiency compared to a system with liquid bulk [equation (17)]. Variation of various system parameters over a wide range showed that Table 1 is valid for any value of k_l, m_a, $[A]_g$, $[A]_l^0$, D_a and v_y (plug flow velocity profile).

It is found (Table 1) that the mass transfer flux decreases with decreasing layer thickness. If the layer has a thickness of at least the penetration depth ($\delta > d_{pen}$) the mass transfer flux approaches a value that corresponds to the mass transfer flux according to the penetration theory ($J_{a,dpen} = J_{a,bulk}$).

If species A penetrates so deeply into the liquid layer during the available contact period that it reaches the solid contact interface, it can not pass the contact surface and the penetrated molecules will collect in the liquid layer. The build up of these molecules results in an increasing liquid phase concentration of species A, thus reducing the effective driving force. As a result, the gradient of species A at the gas–liquid interface will decrease and also the average mass transfer flux during the contact period will decrease (equations (12) and (16)]. This is visualized by comparing Figures 3, 4 and 5, where the time dependent solution of the penetration and layer model is given and from which the mass transfer flux can be obtained using equation (15)

Table 1. Mass transfer efficiency compared to system with liquid bulk, results are valid for physical absorption (plug flow profile).

η_{dpen}	$\eta_{dpen/2}$	$\eta_{dpen/4}$	$\eta_{dpen/8}$	$\eta_{dpen/16}$
1.00	0.82	0.44	0.22	0.11

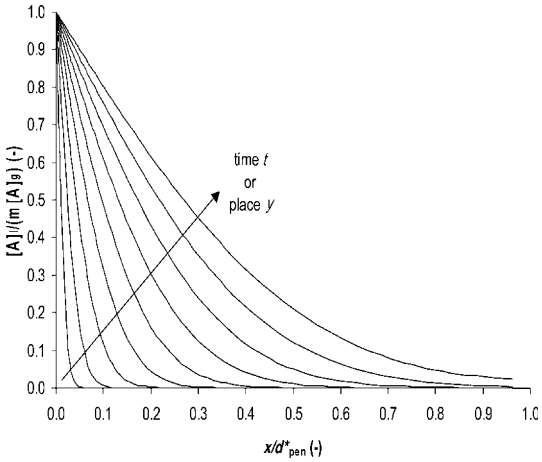

Figure 3. Concentration profiles for basecase with liquid bulk.

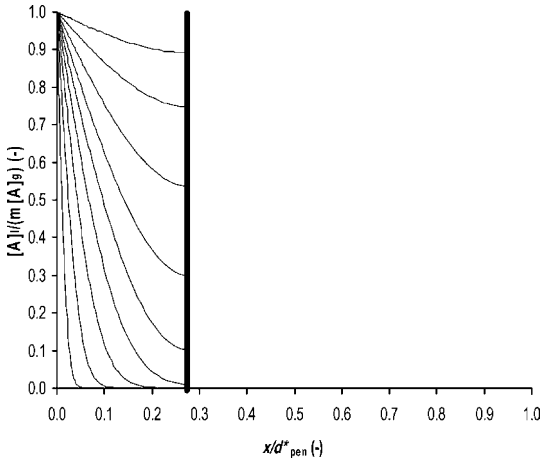

Figure 5. Concentration profiles for basecase with $\delta = d_{pen}/2$.

or (16). In Figure 3 the concentration profiles during the absorption period are shown for a system with liquid bulk. In Figure 4 the same parameters have been used for a system without liquid bulk and a liquid layer with a thickness d_{pen}. In Figure 4 it can be seen that for the last three lines species A starts to build up in the liquid layer (please note that d_{pen} is somewhat smaller than the actual physical penetration depth d^*_{pen}). The influence on the mass transfer flux can however still be neglected since the gradient of the lines at the gas–liquid interface ($x = 0$) is still almost equal to that shown in Figure 3. In Figure 5 the layer thickness has been reduced to $d_{pen}/2$. Now, the gradient of the lines at $x = 0$ is significantly smaller so that the mass transfer flux will decrease (see also Table 1).

This is also shown in Figure 6, where the cumulative flux of the layer model during the contact period is plotted (vertical axis) against the cumulative flux of the penetration model (horizontal axis). Initially, the cumulative flux is independent of the layer thickness (lower left corner of Figure 6) and at a certain moment, depending on the layer thickness, the flux of the layer model falls behind that of the penetration model.

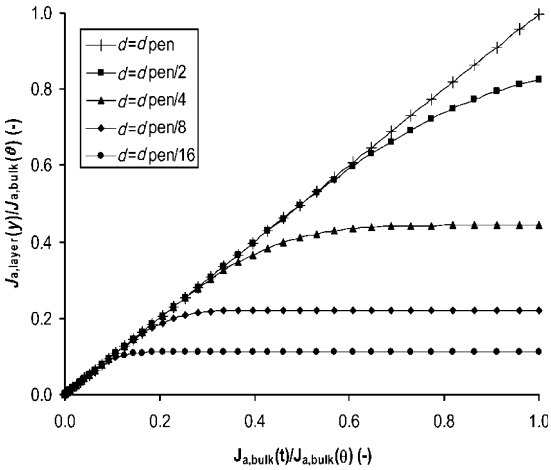

Figure 6. Cumulative (scaled) contribution of mass transfer flux with layer model versus bulk model at various layer thickness, plug flow velocity profile.

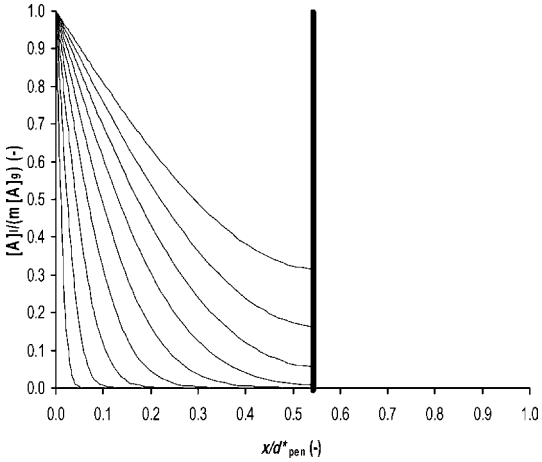

Figure 4. Concentration profiles for basecase with $\delta = d_{pen}$.

The only parameters influencing the results presented in Table 1 are the occurrence of a chemical reaction and the shape of the velocity profile. In case of a fully developed parabolic velocity profile, the results are as given in Table 2.

Comparing Tables 1 and 2 shows that the mass transfer efficiency (and thus the absolute mass transfer) with a parabolic velocity profile is lower than with a plug flow velocity profile. A possible explanation is that with a parabolic velocity profile the liquid layer will move more slowly close to the solid contact surface. This results in a larger accumulation of species A close to the solid contact surface (close to $y = \delta$) and thus lowers the driving force and the mass transfer flux.

Table 2. Mass transfer efficiency compared to system with liquid bulk, results are valid for physical absorption (parabolic flow profile).

η_{dpen}	η_{dpen}	$\eta_{dpen/2}$	$\eta_{dpen/4}$	$\eta_{dpen/8}$	$\eta_{dpen/16}$
0.99	0.92	0.59	0.30	0.15	0.07

It is found (Table 2) that if the layer has a thickness of at least the physical penetration depth ($\delta > d^*_{pen}$) the mass transfer flux approaches a maximum that corresponds to the mass transfer flux according to the penetration theory. If the liquid layer has a thickness above this, species A will not at all reach the solid contact surface and the flux will not be affected by it.

The fact that in case of a plug flow velocity profile the minimum required thickness (d_{pen}) is somewhat less than for a parabolic profile ($d^*_{pen} = d_{pen} \cdot \sqrt{\pi}$) is caused by the fact that although species A does reach the contact surface during the contact period and although species A starts to build up in the liquid layer, the gradient at the gas–liquid interface is not significantly affected and especially the average gradient is not changing significantly in case of plug flow (Figure 4) but does change in case of a parabolic profile (Figure 7). This is also found by comparing the cumulative flux for parabolic flow (Figure 8) and plug flow (Figure 6).

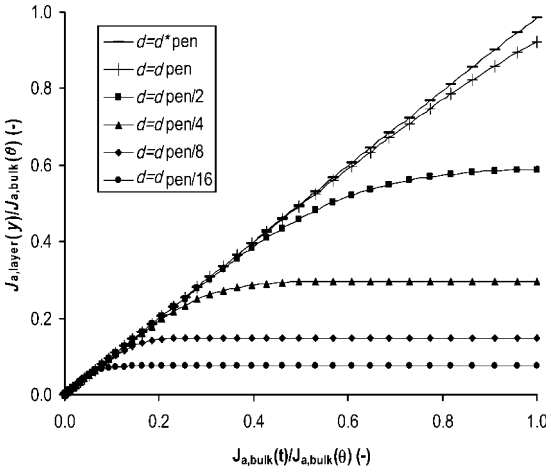

Figure 8. Cumulative (scaled) contribution of mass transfer flux with layer model versus bulk model at various layer thickness, parabolic velocity profile.

Absorption and Irreversible 1,0-Reaction

Absorption can be accompanied by a chemical reaction. In case of an irreversible 1,0-reaction, species A is converted to one or more products (C and D):

$$A(g) \rightarrow A(l) \rightarrow \gamma_c C(l) + \gamma_d D(l) \quad (22)$$

$$R_a = k_R[A] \quad (23)$$

An important parameter that characterises how the mass transfer is affected by the chemical reaction is the reaction-diffusion modulus [Hatta number (Hatta, 1932)]:

$$Ha = \frac{\sqrt{k_R D_a}}{k_l} \quad (24)$$

For systems with bulk, the 'fast reactions' ($Ha > 2$) are considered to proceed predominantly near the gas–liquid interface, while the 'slow reactions' ($Ha < 0.2$) are considered to occur mainly in the liquid bulk. Based on this, it can be expected that the differences between the mass transfer flux for systems with bulk and systems with a liquid layer are most important at low Hatta numbers.

To confirm this, the mass transfer efficiency was determined as a function of Hatta number and layer thickness. It was found that the results do not depend on k_l, m_a, $[A]_g$, D_a and v_y (plug flow velocity profile). The reaction kinetics (k_R) do influence the results and this is included in the results using the dimensionless *Ha* number (Figure 9).

With increasing reaction rate (increasing *Ha*) the minimum required layer thickness for optimal mass transfer ($\eta = 1$) decreases. For example, for $Ha = 0.1$ a layer with a thickness of d_{pen} is required to obtain an efficiency of 1.0. For $Ha = 10$ a layer with a thickness of only $d_{pen}/8$ is sufficient. This can be explained by the fact that with increasing reaction rate, the effective penetration depth of species A decreases because more molecules have been converted into products C and D before they reach the solid contact surface.

Again, in case of plug flow velocity profile, a layer thickness of at least d_{pen} ensures a mass transfer flux equal to that of a system with liquid bulk, for any *Ha*.

The parameter $[A]_l^0$ also influences the results and this is included in the results using the dimensionless number *Sat*. A saturation of 80% means for example that the liquid layer was initially loaded with gas phase species A to an amount

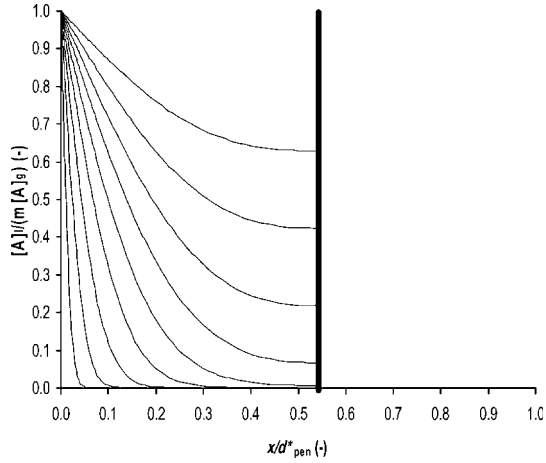

Figure 7. Concentration profiles for basecase with $\delta = d_{pen}$ and parabolic velocity profile.

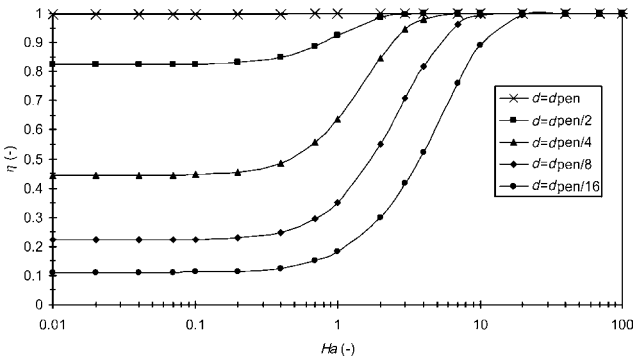

Figure 9. Mass transfer efficiency relative to system with liquid bulk. First order reaction, initially clean liquid, plug flow velocity profile.

of 80% of the saturation capacity [equation (20)]. It is found that the initial saturation of the liquid layer (*Sat*) has an influence on the efficiency factor for Hatta numbers from approximately 0.1 to 2.0 (Figure 10). For these Hatta numbers, the efficiency factor increases with the amount of initial saturation. To explain this result, the three different regions have to be discussed separately. For low Hatta numbers ($Ha < 0.1$) the mass transfer flux decreases linear with (1-*Sat*), this will be the same for systems with and without liquid bulk, so that the efficiency is not dependent of *Sat*. For high Hatta numbers ($Ha > 2$) the reaction is so fast that the saturation decreases to zero very fast and the initial saturation (*Sat*) does not at all influence the flux. Again, the efficiency is not a function of *Sat*. In the intermediate region ($0.1 < Ha < 2$) the situation is more complex, the flux is dependent of *Sat*, but varies not linearly with (1-*Sat*). In this region, the mass transfer is affected by the chemical reaction as well as the diffusion process. The diffusion process itself is however influenced by the presence of the solid contact surface as well as by the value of *Sat*. As can be seen from Figure 10 this becomes more important with decreasing layer thickness (the relative difference in efficiency between a saturation of 0% and 95% increases with decreasing layer thickness, see Table 3).

In case of a fully developed parabolic velocity profile, a similar plot is obtained (Figure 11). A layer thickness of at least d^*_{pen} is required to ensure a mass transfer flux equal to that of a system with liquid bulk, for all Hatta numbers.

Again, the influence of pre-saturating the liquid was investigated (Figure 12). It can be seen that in case of a parabolic velocity profile the mass transfer flux of an initially partially saturated liquid can in theory be higher in case of a liquid layer with thickness of $d_{pen}/2$ than for a system with liquid bulk (an efficiency of 1.13 is found for a 95% saturated liquid layer at $Ha = 0.4$). This can be explained by the fact that for these conditions, the liquid is initially containing more of species A then it does after the contact period. In other words, at $t = 0$ the value of *Sat* is so high that species A is consumed faster than it is transferred from the gas phase to the liquid phase. The chemical reaction enhances the mass transfer, and this influence is favoured by the parabolic velocity profile due to extra refreshment near the gas–liquid interface. For thinner liquid layers this becomes more important because dv_y/dx is larger. Please note that this is not of practical importance because in practice the liquid will initially never be saturated so much that the consumption of A is higher than the transport of A to the liquid.

Table 3. Relative influence of initial saturation on mass transfer efficiency as a function of layer thickness (plug flow, $Ha = 0.4$).

	d_{pen}	$d_{pen}/2$	$d_{pen}/4$	$d_{pen}/8$	$d_{pen}/16$
$\eta_{Sat\ =0\%}$	1.00	0.848	0.485	0.248	0.125
$\eta_{Sat=95\%}$	1.00	0.905	0.583	0.311	0.158
$\frac{\eta_{Sat=95\%}}{\eta_{Sat=0\%}}$	1.00	1.07	1.20	1.25	1.26

Absorption and Irreversible 1,1-Reaction

In case of an irreversible 1,1-reaction, species A and B are converted in the liquid phase into one or more products (C and D):

$$A(g) \longrightarrow A(l); A(l) + B(l) \longrightarrow \gamma_c C(l) + \gamma_d D(l) \tag{25}$$

$$R_a = k_R[A][B] \tag{26}$$

$$Ha = \frac{\sqrt{k_R[B]D_a}}{k_l} \tag{27}$$

In case of a 1,1-reaction, not only species A has to diffuse in the liquid layer, but also species B. This introduces an extra parameter, the maximum enhancement factor, which is approximately given by

$$E_{a\infty} \cong \left(1 + \frac{D_b[B]_{bulk}}{\gamma_b D_a [A]_i}\right)\sqrt{\frac{D_a}{D_b}} \tag{28}$$

Equation (27) is based in the assumption of a pseudo-first order chemical reaction and equation (28) is representing a limit of the enhancement factor due to an instantaneous chemical reaction (Westerterp *et al.*, 1990). The region with 'fast reaction' ($Ha > 2$) can be divided in three separate regions. The first region ($2 < Ha << E_{a\infty}$) where the mass transfer is enhanced by chemical reaction, but where the supply of species B is not a limiting factor. The second region ($Ha >> E_{a\infty}$) where the supply of species B is a limiting factor. The third region is the intermediate area ($Ha \approx E_{a\infty}$) where a transformation from the first regime to the second regime takes place.

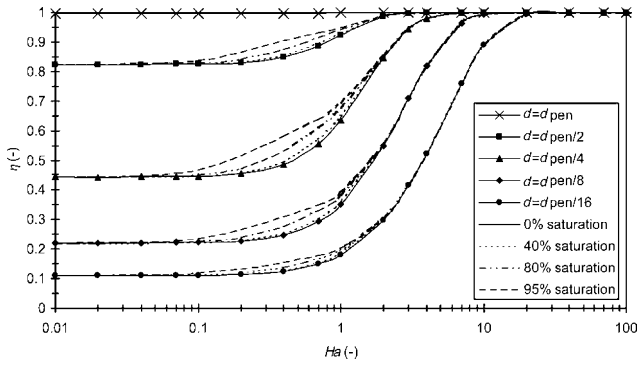

Figure 10. Mass transfer efficiency relative to system with liquid bulk. First order reaction, plug flow velocity profile.

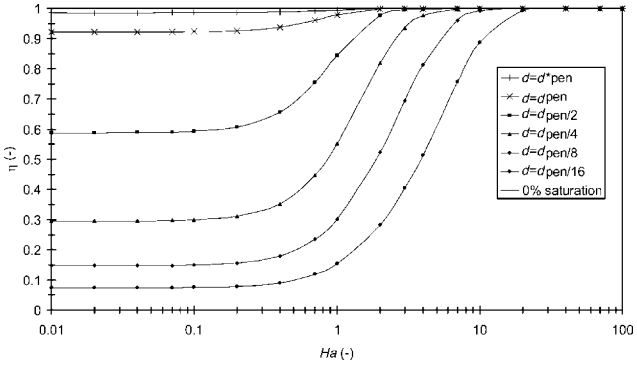

Figure 11. Mass transfer efficiency relative to system with liquid bulk. First order reaction, initially clean liquid, parabolic velocity profile.

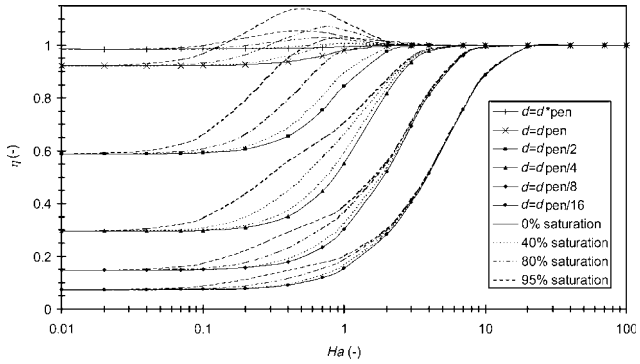

Figure 12. Mass transfer efficiency relative to system with liquid bulk. First order reaction, parabolic velocity profile.

In case of a liquid layer, there is no bulk concentration of B and the following expression was used:

$$E_{a\infty} \cong \left(1 + \frac{D_b[B]^0}{\gamma_b D_a [A]_i}\right)\sqrt{\frac{D_a}{D_b}} \tag{29}$$

Again the mass transfer efficiency was determined as a function of Hatta number and layer thickness. It was found that the results depend on the value of $E_{a\infty}$. It was also found that there is a difference in the results obtained when $D_a = D_b$ and when $D_a \neq D_b$.

In Figures 13 and 15 (plug flow respectively parabolic flow) the results are shown obtained when $D_a = D_b$ and $E_{a\infty} = 21$. Comparing Figure 13 with Figure 10 and Figure 15 with Figure 12, it is clear that the left-hand sides ($Ha < 0.2$) of the plots are identical. For $Ha > 0.2$ the mass transfer efficiency of the 1,1-reaction drops compared to the efficiency of the 1,0-reaction for equal layer thickness. However, as long as $Ha << E_{a\infty}$, the differences are small.

It is interesting to see that at a Hatta number of approximately 4, a maximum efficiency is found and the efficiency starts to drop with increasing Hatta number. This is caused by the supply of species B that becomes a limiting factor. Due to the absence of a liquid bulk the amount of species B available is limited, the concentration of B drops as well as the reaction rate. The reduced reaction rate puts a limit on the chemical enhancement of mass transfer.

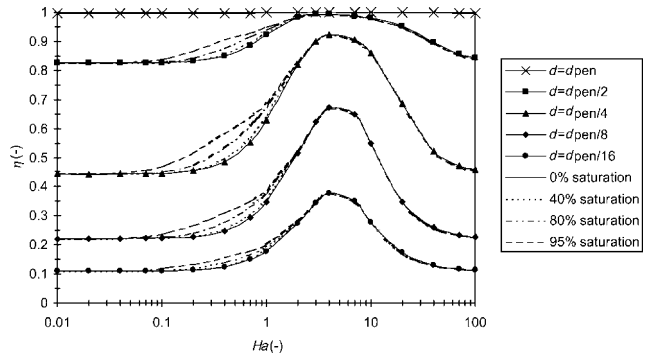

Figure 13. Mass transfer efficiency relative to system with liquid bulk. Second order reaction, plug flow velocity profile, $D_a = D_b$, $E_{a\infty} = 21$.

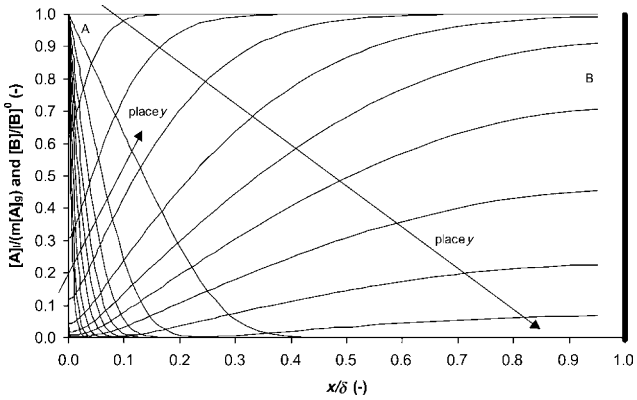

Figure 14. Concentration profiles corresponding to Figure 13 for $Ha = 200$ with $\delta = d_{pen}/2$.

When further increasing the Hatta number, the mass transfer efficiency approaches a limit again once $Ha >> E_{a\infty}$. In case $D_a = D_b$ this limit is equal to the limit for $Ha < 0.2$. The reason for this limit is that the mass transfer fluxes do no longer change with increasing Hatta number because the supply of B has completely limited the chemical enhancement of mass transfer. This can be seen from Figure 14, where it is shown that species B is almost exhausted at position x reached by species A.

To understand the influence of $E_{a\infty}$, the calculations have been repeated at various values of $E_{a\infty}$. Some of the results are shown in Figure 16. It can be seen that with increasing $E_{a\infty}$, the similarity with the results obtained for a 1,0-reaction (Figure 9) holds out till higher Hatta numbers. Also, the required Hatta number to reach the right-hand side limit increases with $E_{a\infty}$ because this limit is reached for $Ha >> E_{a\infty}$.

Finally, we looked at the effect of changing the ratio between D_a and D_b. To keep the value of $E_{a\infty}$ for the reference system with liquid bulk the same, also the concentration of species B was adjusted, so that $E_{a\infty}$ did not change. The results are shown in Figures 17 and 18. Again, the left-hand side of the plots is not changing and for $Ha < 0.2$ an efficiency of 1.0 is obtained if the condition $\delta \geq d_{pen}$ is fulfilled (Figure 13). In the right-hand side of the plots it can however be seen that the right limit changes with the ratio D_a/D_b. It can also be seen that with increasing D_a/D_b the plot becomes identical with the plot of a 1,0-reaction system (Figure 9).

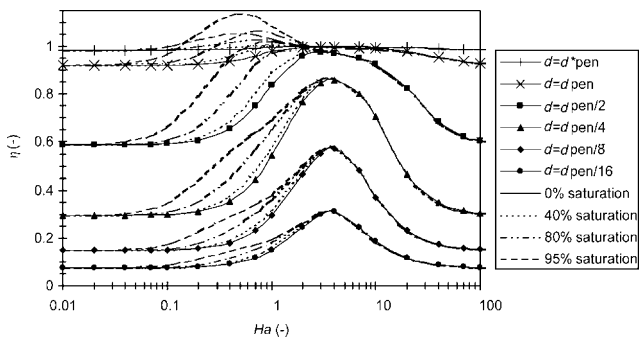

Figure 15. Mass transfer efficiency relative to system with liquid bulk. Second order reaction, parabolic velocity profile, $D_a = D_b$, $E_{a\infty} = 21$.

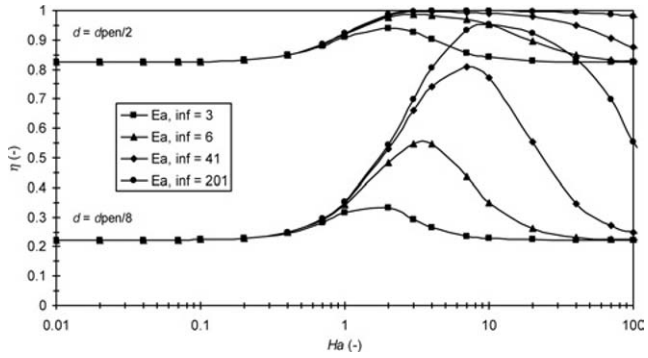

Figure 16. Mass transfer efficiency relative to system with liquid bulk. Second order reaction, plug flow velocity profile, $D_a = D_b$, $Sat = 0$.

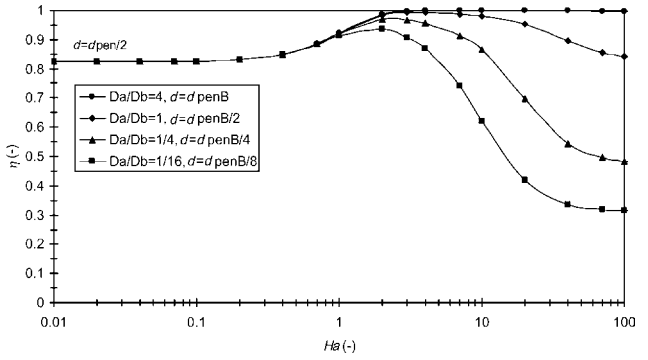

Figure 17. Mass transfer efficiency relative to system with liquid bulk. Second order reaction, plug flow velocity profile, $E_{a\infty} = 21$, $Sat = 0$, $d = d_{pen}/2$.

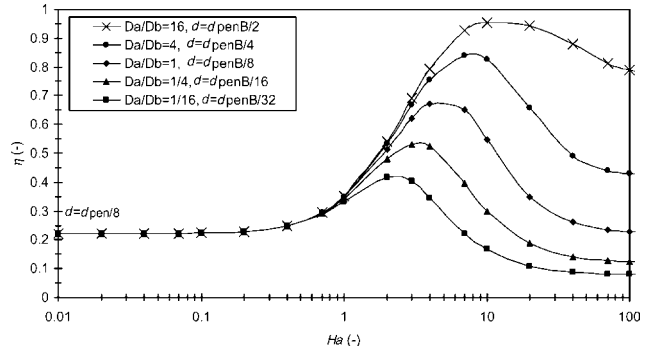

Figure 18. Mass transfer efficiency relative to system with liquid bulk. Second order reaction, plug flow velocity profile, $E_{a\infty} = 21$, $Sat = 0$, $d = d_{pen}/8$.

DESIGN IMPLICATIONS

The criteria found for successful application of the penetration model are summarized in Table 4.

To understand the impact of the criteria presented above on equipment design let's consider an absorption column with structured packing. The Sherwood number for mass transfer is defined as

$$Sh = \frac{k_l \delta}{D_a} \tag{30}$$

Table 4. Operation window of the penetration model.

Absorption	Flow	Hatta	Operation window
Physical	Plug	—	$\delta \geq d_{pen}$
Physical	Parabolic	—	$\delta \geq d^*_{pen}$
1,0-reaction	Plug	Any	$\delta \geq d_{pen}$
1,0 reaction	Parabolic	Any	$\delta \geq d^*_{pen}$
1,1-reaction	Plug	< 0.2	$\delta \geq d_{pen}$
1,1-reaction	Plug	$>> E_{a\infty}$	$\delta \geq d_{pen,b}$
1,1-reaction	Plug	Any	$\delta \geq d_{pen}$ and $\delta \geq d_{pen,b}$
1,1-reaction	Parabolic	< 0.2	$\delta \geq d^*_{pen}$
1,1-reaction	Parabolic	$>> E_{a\infty}$	$\delta \geq d^*_{pen,b}$
1,1-reaction	Parabolic	Any	$\delta \geq d^*_{pen}$ and $\delta \geq d^*_{pen,b}$

Table 5. Operation window of the penetration model in terms of Sh (packed column).

Absorption	Operation window
Physical	$Sh \geq 4$ (or $Fo < 1/4\pi$)
1,0-reaction, with any *Ha*	
1,1-reaction, with $Ha < 0.2$	
1,1-reaction, with any *Ha*	$Sh \geq 4$ and $Sh \geq 4\sqrt{D_b/D_a}$

In Table 4, the criteria for parabolic flow are stricter than for plug flow. In practice a system will be in between plug flow and parabolic flow, so that the criteria for parabolic flow should be chosen. Combination of equation (30) and Table 4 gives the final operation window in terms of Sherwood number as shown in Table 5.

Typical Sherwood numbers for packed columns are 10–100 (Westerterp *et al.*, 1990). From this we can conclude that for most practical applications there is no need to use the layer model instead of the penetration model. Special attention is required in case of by 1,1-reactions enhanced mass transfer in combination with low Sherwood numbers and $D_b >> D_a$.

CONCLUSIONS

Existing micro models for gas–liquid mass transfer assume the presence of a liquid bulk. Strictly, this means that they can only be applied provided that a liquid bulk is available. The calculations in this paper indicate that application of the penetration model is in many situations also possible for systems without liquid bulk.

If a thin layer of liquid flows down over a solid contact surface, the penetration model will give good results as long as the layer thickness δ is at least equal to the penetration depth d^*_{pen}. In terms of Sherwood number this means $Sh \geq 4$. In case of a 1,1-reaction with $Ha > 0.2$ a second criterion is $Sh \geq 4\sqrt{D_b/D_a}$ If this condition is not fulfilled, the penetration model may predict too optimistic values for the mass transfer flux.

NOMENCLATURE

d	film or layer thickness, m
d_{pen}	effective physical penetration depth of species A for plug flow profile (defined by $\sqrt{4D_a\theta}$), m
$d_{pen,subscript}$	effective physical penetration depth for plug flow velocity profile (defined by $\sqrt{4D_{subscript}\theta}$), m
d^*_{pen}	actual physical penetration depth (defined by dpen $\cdot \sqrt{\pi}$).

$D_{subscript}$	diffusivity, $m^2\ s^{-1}$
E_a	enhancement factor, 1
$E_{a,\infty}$	enhancement factor instantaneous reaction, 1
Fo	Fourier number, 1
g	gravitational constant, $m\ s^{-2}$
Ha	Hatta number [defined by equation (19)], 1
$J_{subscript}$	molar flux, $mol\ m^{-2}\ s^{-1}$
$J_{a,subscript}$	molar flux of species A, the subscript defines the layer thickness δ, $mol\ m^{-2}\ s^{-1}$
$k_{subscript}$	mass transfer coefficient, $m\ s^{-1}$
k_R	reaction rate constant, $m^{3q}\ mol^{-q}\ s^{-1}$
L	contact length (defined by $v_y\theta$), m
$m_{subscript}$	gas–liquid partition coefficient, l
n	reaction order of species B, 1
$R_{subscript}$	reaction rate, $mol\ m^{-3}\ s^{-1}$
R_{gas}	ideal gas constant, $J\ mol^{-1}\ K^{-1}$
Sat	saturation liquid by component A [equation (20)], 1
Sh	Sherwood number [defined by equation (30)], 1
t	time variable, s
$v_{subscript}$	velocity, $m\ s^{-1}$
x	position perpendicular to interface, m
X	dimensionless layer thickness [equation (18)], m
y	position parallel to interface, m
$[]_{subscript}$	concentration at position subscript, $mol\ m^{-3}$
δ	film or layer thickness, m
γ	stoichiometric constant, 1
μ	dynamic viscosity, Pa s
η	efficiency compared to system with liquid bulk (relative flux) [defined by equation (17)], 1
ρ	density, $kg\ m^{-3}$
θ	contact time according to penetration model (defined by $4D_a/\pi k_l^2$), s

Subscripts

0	initial value
a,b,c,d	of respectively species A, B, C or D
bulk	at bulk conditions
g	gas phase
i	interface
i	species i
l	liquid phase
layer	for systems without liquid bulk
pen	according to penetration theory
x/y	in *x* direction/in *y* direction

REFERENCES

Danckwerts, P.V., 1951, Significance of liquid-film coefficients in gas absorption, *Ind Eng Chem*, 43: 1460–1467.

Dobbins, W.E., 1956, in McCable, M.L. and Eckenfelder, W.W., (Eds.). *Biological Treatment of Sewage and Industrial Wastes, Part 2-1*, (Reinhold, New York, USA).

Hatta, S., 1932, On the absorption velocity of gases by liquids, *Tech Rep Tohoku Imp Univ*, 10: 119–135.

Higbie, R., 1935, The rate of absorption of a pure gas into a still liquid during short periods of exposure, *Trans Am Inst Chem Eng*, 35: 36–60.

Toor, H.L. and Marchello, J.M., 1958, Film-penetration model for mass transfer and heat transfer, *AIChE* 4: 97–101.

Versteeg, G.F., Kuipers, J.A.M., van Beckum, F.P.H. and van, Swaaij, W.P.M., 1989, Mass transfer with complex reversible chemical reactions—I. Single reversible chemical reaction, *Chem Eng Sci*, 44: 2295–2310.

Westerterp, K.R., van Swaaij, W.P.M. and Beenackers, A.A.C.M., 1990, *Chemical Reactor Design and Operation* (Wiley, New York, USA).

Whitman, W.G., 1923, Preliminary experimental confirmation of the two-film theory of gas absorption, *Chem Metall Eng*, 29: 146–148.

The manuscript was received 28 June 2006 and accepted for publication after revision 19 December 2006.